forests

MDPI

Article

Cupressaceae Pollen in the City of Évora, South of Portugal: Disruption of the Pollen during Air Transport Facilitates Allergen Exposure

Ana Galveias [1], Ana R. Costa [1], Daniele Bortoli [2,3], Russell Alpizar-Jara [4], Rui Salgado [2,3], Maria João Costa [2,3] and Célia M. Antunes [1,*]

[1] Department of Chemistry, ICT—Institute of Earth Sciences, School of Sciences and Technology & IIFA, University of Évora, 7000-671 Évora, Portugal; acgjorge@uevora.pt (A.G.); acrc@uevora.pt (A.R.C.)
[2] Department of Physics, ICT—Institute of Earth Sciences, School of Sciences and Technology & IIFA, University of Évora, 7000-671 Évora, Portugal; db@uevora.pt (D.B.); rsal@uevora.pt (R.S.); mjcosta@uevora.pt (M.J.C.)
[3] EaRSLab—Earth Remote Sensing Laboratory, University of Évora, 7000-671 Évora, Portugal
[4] CIMA—Research Center of Mathematics and Applications & Department of Mathematics, School of Sciences and Technology, University of Évora, 7000-671 Évora, Portugal; alpizar@uevora.pt
* Correspondence: cmma@uevora.pt; Tel.: +35-12-6674-5311

Abstract: Research Highlights: Daily airborne Cupressaceae pollen disruption ranged from 20 to 90%; relative humidity (RH), rainfall and atmospheric pressure (AtP) were the major meteorological determinants of this phenomenon. *Background and Objectives:* Cupressaceae family includes several species that are widely used as ornamental plants pollinating in late winter-early spring and might be responsible for allergic outbreaks. Cupressaceae pollen disruption may favour allergen dissemination, potentiating its allergenicity. The aim of this work was to characterize the Cupressaceae pollen aerobiology in Évora, South of Portugal, in 2017 and 2018, particularly the pollen disruption, and to identify the meteorological parameters contributing to this phenomenon. *Materials and Methods:* Pollen was collected using a Hirst type 7-day pollen trap and was identified following the standard methodology. Temperature, RH, rainfall, global solar radiation (Global Srad), AtP, wind speed and direction were obtained from a weather station installed side-by-side to the Hirst platform. Back trajectories (12-h) of air masses arriving at Évora were calculated using the HYSPLIT model. *Results:* Cupressaceae pollen index was higher in 2017 compared to 2018 (>5994 and 3175 pollen/m^3, respectively) and 36 ± 19% (2017) and 64 ± 17% (2018) of the pollen was disrupted. Higher levels of disrupted pollen coincided with RH > 60% and rainfall. Temperature, Global Srad and AtP correlated negatively with pollen disruption. Wind speed and wind direction did not significantly correlate with pollen disruption. Intra-diurnal pollen pattern peaked between 9:00 am–2:00 pm, suggesting local origin, confirmed by the back trajectory analysis. Intra-diurnal pollen disruption profile followed hourly pollen pattern and it negatively correlated with AtP, temperature and Global Srad but was uncorrelated with RH. *Conclusions:* The results suggest that RH, rainfall and AtP are the main factors affecting airborne Cupressaceae pollen integrity and in conjunction with daily pollen concentration may be used to predict the risk of allergy outbreaks to this pollen type.

Keywords: Cupressaceae pollen; pollen disruption; meteorological parameters; back trajectories

Citation: Galveias, A.; Costa, A.R.; Bortoli, D.; Alpizar-Jara, R.; Salgado, R.; Costa, M.J.; Antunes, C.M. Cupressaceae Pollen in the City of Évora, South of Portugal: Disruption of the Pollen during Air Transport Facilitates Allergen Exposure. *Forests* **2021**, *12*, 64. https://doi.org/10.3390/f12010064

Received: 30 November 2020
Accepted: 2 January 2021
Published: 8 January 2021

1. Introduction

The Cupressaceae is a cosmopolitan family and the second most important family of Gymnosperms [1–3]. The family includes 30 genera and 160 species distributed by temperate or temperate-warm regions of Northern and Southern Hemispheres, although almost 3/4 of the species are present in the Northern hemisphere [1,3]. They are coniferous and heliophiles plants, with medium size, and can grow up to 30 m maximum. Cupressaceae is the only family that shows a non-spiral arrangement of microsporophylls and

each microsporophyll bears a variable number (2–6) of pollen bags [2]. Currently, this family is distributed in all of Earth's continents, except Antarctica. In the Iberian Peninsula, species from the genus *Juniperus* form part of the natural vegetation and the scrubland and are considered autochthonous while species from the genera *Cupressus*, *Chamaecyparis* and *Platycladus*, widely used in parks and gardens as barriers against wind and noise, are considered allochthonous [4]. In Portugal, several species from the genera *Juniperus* and *Cupressus* are distributed throughout the continental territory, and *Cryptomeria*, particularly *Cryptomeria japonica*, is abundant in the Azores islands [5]. Among the several autochthones species from the genus *Juniperus*, the *Juniperus communis* L., *Juniperus navicularis* Gand., *Juniperus oxycedrus* L. and *Juniperus turbinata* Guss are well represented [6]. The genus *Cupressus*, is considered allochthonous in Portugal and is distributed throughout the country; the species *Cupressus sempervirens* L. is mainly found in urban environments, due to its use as ornamental plants, *Cupressus macrocarpa* Hartweg is usually found in mountains of Sintra, Buçaco and Geres, and *Cupressus lusitanica* Miller is found both environments; the distribution of *Cupressus arizonica* Greene is mostly unknown [6,7].

The pollination of *Cupressaceae* trees is anemophilous and occurs from late winter to early spring and may last for more than a month, due to its microsporophyll gradual maturation mechanism, from bottom to top of the flower [8,9]. Due to the large number of trees from these species in habitational areas or surroundings in Portugal, particularly the species *Cupressus sempervirens* and *Cupressus lusitanica* as a result of their use as ornamental plants [6,7], there is a high production and release of pollen into the atmosphere [8,10–12], which causes an increase in the Cupressaceae pollen allergen availability in breathing air [13–15] and an allergenic risk associated with these exposure [16,17].

Meteorological parameters are crucial factors influencing plant physiology and consequently pollen release dynamics. Temperature has an important role in maturation and flowering and is the factor that most influences the growth and development of plants and pollen production. Typically, anthers of the gymnosperm plants open when the relative humidity decreases, below 80%, and the temperature increases [18], allowing anemophilous pollen dispersal. Daily airborne pollen typically follows a dynamic pattern, that can be achieved by hourly accounts [19], with maximal concentrations in the atmosphere observed when temperature rises in the morning [10,20]. On the contrary, rain seems to develop a negative effect, contributing to a reduction of pollen in the atmosphere [21], probably by a washout effect, inducing the deposition of pollen [22].

Researchers have long believed that meteorological changes can cause loss of pollen and spore integrity, forming and releasing smaller particles to the surrounding environment. Pollen disruption in the anthers was observed in grasses and in birch inflorescences, caused by water or by a high humidity environment [23,24] as well as in atmosphere [24] but the meteorological factors affecting airborne pollen disruption is not yet fully understood. Moreover, to our knowledge the characterization of airborne pollen disruption on the Cupressaceae family has not yet been reported.

This phenomenon allows the release of the allergen content to ambient air enhancing its availability for inhalation. In fact, cycles of wetting and drying followed by wind disturbance originated aerosol particles in the size range 0.12 to 4.67 μm, where major allergens were identified [23]. Also, Ole e 1 allergen was detected not only in the PM > 10 μm fraction, associated with pollen, but also in the 10 μm > PM > 2.5-μm fraction [25], showing that small and allergenic particles are present in the atmosphere. Pollen disruption has already been associated with a significantly augmented risk for allergic asthma outbreaks [26]. Cupressaceae is main cause of winter allergic reactions in the southern countries [10] and pollen disruption in the atmosphere might be an important factor aggravating its allergenicity.

In this work we have investigated the disruption of Cupressaceae pollen in a real-world scenario, in the south of Portugal. Data from Cupressaceae airborne pollen and meteorological parameters were collected from the years 2017 and 2018, seeking to elucidate

the effect of meteorological factors on airborne pollen integrity and to identify the most relevant parameters contributing to Cupressaceae pollen disruption in the atmosphere.

2. Materials and Methods

2.1. Study Area and Period

The study focuses on the city of Évora, located in the south of Portugal (Figure 1). Data was collected in the Évora Atmospheric Sciences Observatory (EVASO) of the Institute of Earth Sciences (ICT) at the University of Évora (UE) (38° 34′ N, 7° 54′ W, 293 m asl). Évora is characterized by a temperate climate with warm and dry summers that can be described as Hot-summer Mediterranean climate (Köppen Climate Classification—Csa). According to the climatological normal (1981–2010) provided by the Portuguese Institute for Sea and Atmosphere [27], national authority for climate, the annual mean air temperature is 16.5 °C, with the highest monthly value occurring in August (24.1 °C) and the lowest in January (9.6 °C). The rainfall period, occurring mostly seasonally between October and April, presents an annual precipitation of 585.3 mm.

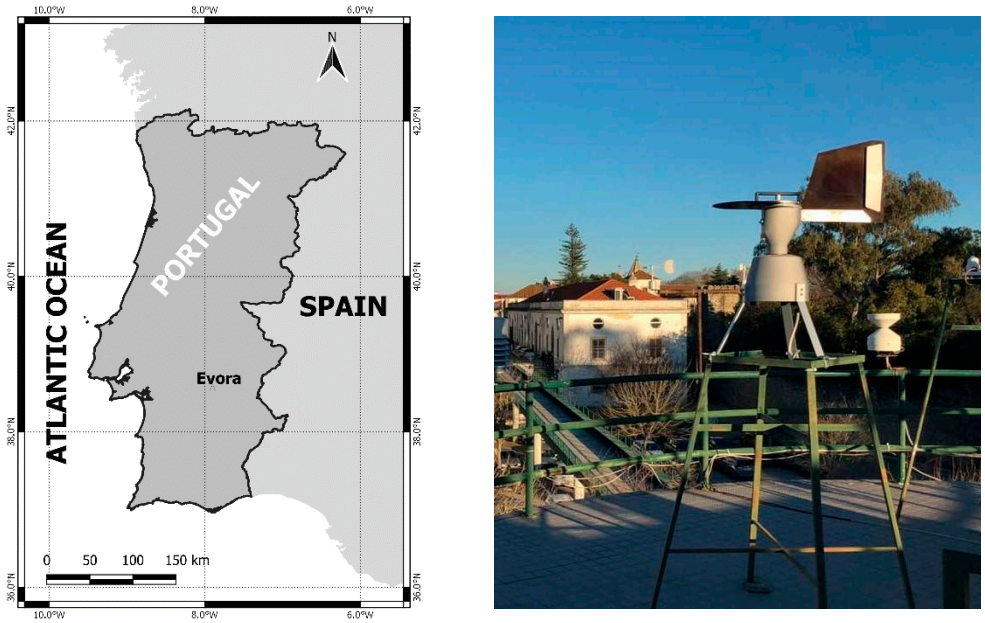

(**a**) (**b**)

Figure 1. Map of Portugal illustrating the location of Évora (**a**) and photo of EVASO where the Hirst type pollen trap and the weather station are installed (**b**).

Cupressaceae pollen are typically detected in large amounts in the south of Portugal during late winter and early spring seasons, particularly, in the months of February and March. The periods selected for the present study comprise three weeks in 2017 and in 2018, from 22 February to 19 March.

2.2. Airborne Pollen Sampling

Airborne Cupressaceae pollen was collected with a Hirst-type volumetric spore trap (Hirst 1952) at EVASO (Figure 1), located on the roof of a building belonging to the University of Évora, approximately 10 m above ground level, since the 22 February 2017. The sampler sucks in air at a rate of 10 L/min, and pollen grains are trapped on an adhesive coated Melinex® strip. Sampling and slide analysis were carried out in accordance with the protocol developed by the European Aeroallergen Network (EAN) and Spanish Aerobiology Network (REA) [28,29]. Slides were analysed daily under a light microscope (400× magnification), with four longitudinal sweeps per slide, according to the standard

method [28,29]. The daily or hourly airborne pollen concentrations were expressed as pollen per cubic meter of air (Pollen/m^3).

The main pollen Season (MPS) was determined by the method of percentage described for Nilsson and Persson, 1981, based on the elimination of a 2.5% percentage in the beginning and end of the pollen season [30,31].

2.3. Meteorological Parameters and Remote Sensing Data

The meteorological parameters used were obtained from the meteorological station installed at EVASO, namely the air temperature (°C), relative humidity (RH; %), precipitation (mm), global solar radiation (W/m^2), wind speed and direction (m/s; °) and atmospheric pressure (AtP; hPa). All variables were measured in 10 s intervals and subsequently averaged to yield hourly and daily values, except for precipitation that is accumulated during the period. The average of the wind direction is obtained applying the arctangent function to the ratio between the mean east-west and the north-south components of wind. The mean east-west and north-south wind components are computed using all the non-zero wind speed samples. This average is done according to the procedure described in the manual of the data logger used in the weather station (CR100) from Campbell Scientific (https://s.campbellsci.com/documents/br/manuals/cr1000.pdf, last accessed 21 December 2020) [32]. Maximum and minimum temperatures are obtained daily. All instruments are subject to periodic checks and maintenance procedures.

The ceilometer is an optical active remote sensing instrument that uses electromagnetic radiation to obtain information about the height where the atmospheric constituent backscatters the radiation. A VAISALA Ceilometer CL31 installed at EVASO since May 2006 provides measurements of the cloud base height up to three simultaneous layers and of the profile of the backscatter coefficient, which in the absence of clouds gives a good approximation of the qualitative aerosol boundary layer profile. This ceilometer has a measurement range from 0 to 7.5 km, with a maximum vertical resolution of 5 m and programmable measurement cycle (from 2 to 120 s). It uses an eye-safe laser InGaAs diode at 910 nm. The ceilometer backscatter measurements are used here as auxiliary data to detect low atmospheric aerosol layers that could be related with pollen occurrences reaching Évora.

2.4. Back Trajectory Analysis

Back trajectories of air masses arriving at Évora have been calculated using the Hybrid Single-Particle Lagrangian Integrated Trajectory model (HYSPLIT). The HYSPLIT model, developed by the National Oceanic and Atmospheric Administration (NOAA), is one of the most widely used and complete models for a simple calculation [33,34]. The meteorological data used for the back trajectory calculations is obtained from the Global Data Assimilation System (GDAS) at a spatial resolution of 0.5°. The vertical motion method used to compute the back trajectories is the model vertical velocity. The back trajectories were calculated for a 24-h period, for every hour of that period, at three different height levels of 100 m, 500 m and 1000 m. The back trajectories obtained for 10:00 UTC are presented in the manuscript, since they are representative of the situation during the rest of the day and in most of the cases a pollen peak is observed around this time. Additionally, the hourly back trajectories are presented in the Supplementary Materials.

2.5. Statistics Analysis

Statistical analysis including non-parametric tests and Pearson's correlation analysis (significance level of 5%) was used to study the relationship between meteorological parameters of maximum, minimum and mean air temperatures, precipitation, RH, global solar radiation, wind speed and direction and AtP (hPa) with disrupted pollen (%).

Statistical assessment of differences was performed using KrusKal-Wallis ($p < 0.05$ was accepted) [35]. Graphs were produced using OriginPro software (OriginLab corporation).

The principal component analysis (PCA) was applied to evaluate the association between the disruption pollen in the air with the meteorological parameters [36].

The mean values shown in the tables and the text represent mean ± standard deviation unless stated otherwise.

3. Results

3.1. Characterization of the Cupressaceae Pollen Season in Évora, South of Portugal

The Cupressaceae pollen was detected in large concentrations in the atmosphere of Évora during winter–spring seasons, particularly, in the months of February and March of 2017 and 2018 with a seasonal pollen index of >5994 (sampling begun on the 22 February 2017) and 3175 pollen/m^3, respectively. The pollen peaked on 25 February 2017 with a concentration of 1635 pollen/m^3 and on 26 February 2018 with a concentration of 644 pollen/m^3.

During the main season, the period of higher concentrations of Cupressaceae pollen occurred from 22 February to 19 March. During this period, 36 ± 19% (2017) and 64 ± 17% (2018) of the pollen that arrived at the collector was disrupted with exine wall rupture, dilatation of the intine wall and release of the cellular content to the environment (Figure 2a,b).

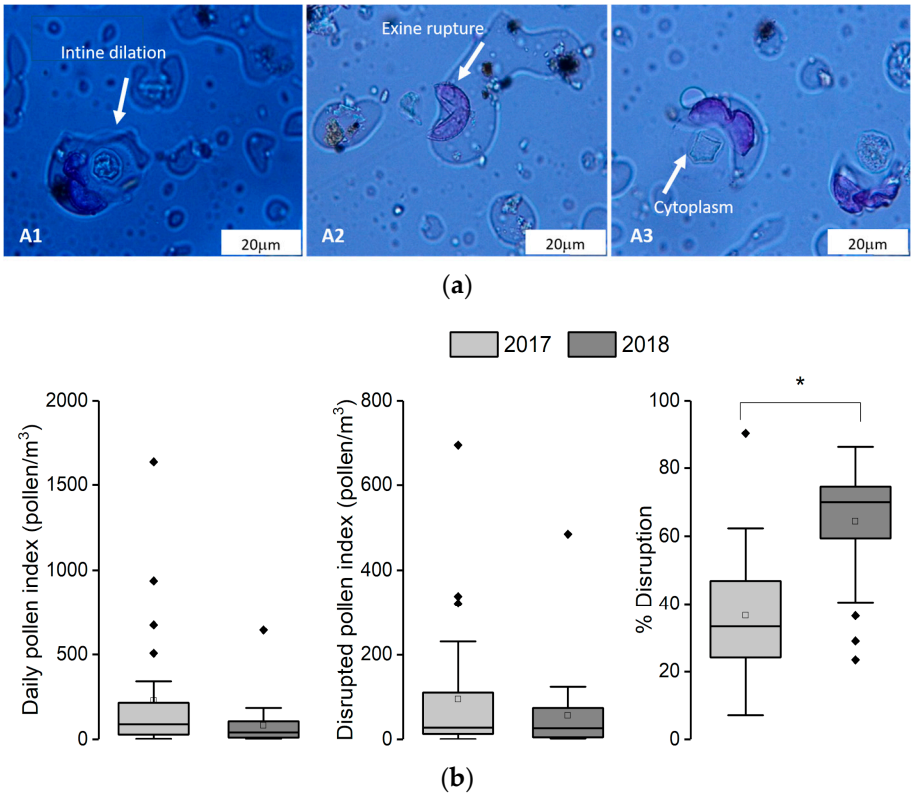

Figure 2. Loss of integrity of Cupressaceae pollen. (**a**) pollen micrographies (with microscopy camera using a 400X amplification). (**b**) daily pollen concentration and pollen disruption (%) in 2017 and 2018 in the studied period. * statistical significance at 5% range ($p < 0.05$).

A linear relationship was found between daily disrupted pollen (DRP) and daily pollen concentration (DPC); when taking the slope of the two years together, which is a measure of the mean ratio DRP/DPC which is 0.45 (0.41–0.48 at 95% confidence) while when considered separately, the slope is 0.42 (0.39–0.44 at 95% confidence) and 0.72 (0.66–0.77 at 95% confidence) for 2017 and 2018, respectively (see Supplementary Materials, Figure S1).

The year 2017 was extremely warm and dry from a climatological point of view, with the south of Portugal affected by drought conditions, which progressively reached severe and extreme drought according to the Portuguese Institute for the Sea and Atmosphere (IPMA; www.ipma.pt, last accessed on 20 December 2020). The situation lasted until the beginning of March 2018, when the occurrence of rainfall relieved the situation [37]. The meteorological conditions prevailing during both years are reflected in the conditions presented for the two periods of study in Table 1. The season was colder and moister in 2018 compared to 2017, as shown by the average seasonal temperatures 2 to 4 °C lower for the maximum (T_{max}), minimum (T_{min}) and mean (T_{mean}) temperatures accompanied by a lower RH in 2017 (Table 1).

Table 1. Values of meteorological parameters at Évora for the years 2017 and 2018 (averaged for the period 22 February to 19 March of each year, except precipitation). ** statistical significance (Stat. sig.) at 1% ($p < 0.01$).

Meteorological Parameters	2017	2018	Stat. Sig.
Maximum temperature, T_{max} (°C)	20.0 ± 3.9	16.43 ± 1.65	$p = 0.0002$ **
Minimum temperature, T_{min} (°C)	10.0 ± 2.2	7.9 ± 2.3	$p = 0.002$ **
Mean temperature, T_{mean} (°C)	14.3 ± 2.8	11.6 ± 1.8	$p = 0.0003$ **
Precipitation (accumulated, mm)	28.3	329.9	-
Relative humidity, RH (%)	63.5 ± 14.2	75.1 ± 15.7	$p = 0.001$ **
Global Solar radiation, Global Srad (W/m^2)	175.0 ± 61.7	130.1 ± 59.6	$p = 0.006$ **
Wind speed, WS (m/s)	2.2 ± 0.9	2.0 ± 0.5	$p = 0.811$
Wind direction, WD (°)	SW-NE	S-W	$p = 0.176$
Atmospheric pressure, AtP (hPa)	986.7 ± 4.3	973.0 ± 6.6	$p = 6.573 \times 10^{-9}$ **

In 2018, the average global solar radiation (Global Srad) was lower, and the precipitation was approximately 12 times higher (Table 1) compared to 2017, in the period considered. The mean wind speed (WS) was similar for both years, but the predominant wind direction (WD) was SW-NE in the year 2017 and S-W in 2018 and average atmospheric pressure (AtP) was slightly lower in 2018 (Table 1).

3.2. Daily Pollen Concentration and Daily Meteorological Parameters Affecting Pollen Integrity

The daily pollen concentration (DPC) was observed to be 2–3 fold higher in 2017 compared to 2018 and the daily ruptured pollen profile followed the DPI, but the level of disrupted pollen was higher in 2018. The number of days with >50% of ruptured pollen were 6 and 19 in 2017 and 2018, respectively (Figure 3a).

Concerning the meteorological parameters, the temperature, accompanied by the Global Srad, tended to increase during the season from February to March in 2017 but not in 2018; in 2018 the temperature and the Global Srad maintained fairly similar values throughout the season (Figure 3b,c). The AtP was above 970 hPa in 2017 during the period considered, while in 2018 it was usually below this value (Figure 3b). The daily RH varied from 50% to 85% in 2017 and from 50% to 95% in 2018 and the number of days with RH > 70% was 10 and 21 in 2017 and 2018, respectively (Figure 3c).

In 2018, rainfall occurred almost every day in the period under analysis (22/26 days), contrarily to 2017 when rainfall only occurred in 6/26 days (Figure 3a). The wind speed was usually below 2 m/s in both years except for a week from 11 to 18 March 2017 when the wind speed reached 5 m/s.

To evaluate the effect of the different meteorological parameters on the pollen disruption, a correlation analysis was performed. The ratio of pollen disruption showed a negative and significant correlation with temperature (T_{max}, T_{mean} and T_{min}), Global Srad

and AtP while it was positively correlated with rainfall and RH (Table 2), where higher disruption is correlated with RH > 60% and with AtP < 980 hPa (Figure 4). Wind speed and wind direction did not significantly correlate with pollen disruption (Table 2). However, the pollen disruption ratio was higher when precipitation occurred (61.0 ± 15.8% and 33.6 ± 24.0%, respectively; $p < 0.05$) (Figure 4).

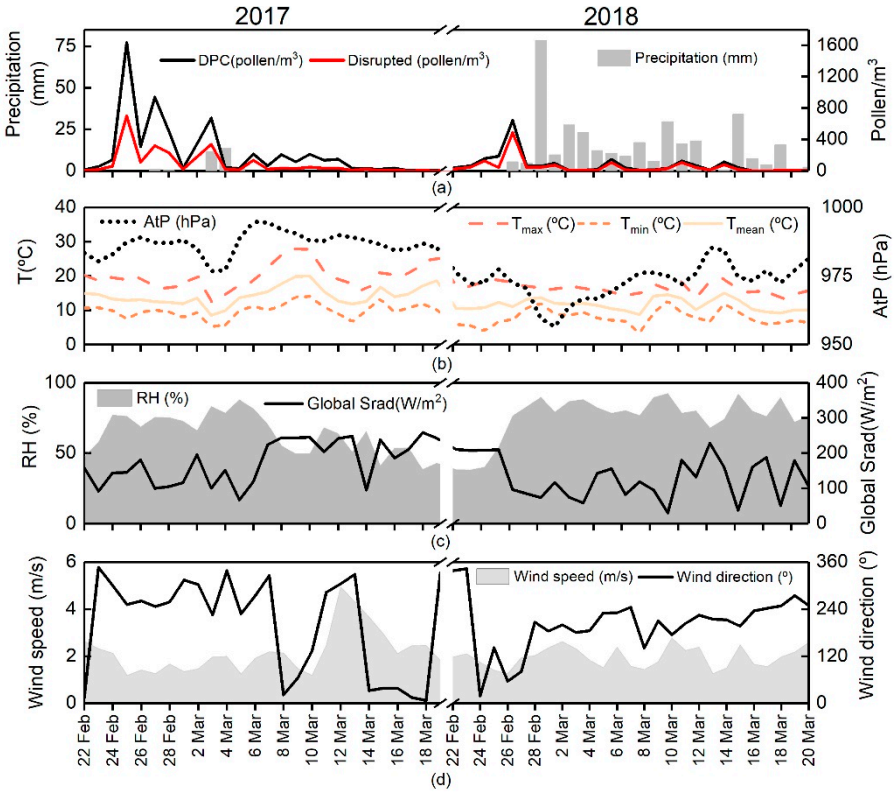

Figure 3. Daily meteorological parameters and daily pollen concentration (DPC), for the period 22 February to 19 March of 2017 and 2018. DPC and rainfall (**a**); daily averaged temperatures (T_{max}, T_{min}, T_{mean}) and atmospheric pressure (**b**); RH and Global Srad (**c**); and wind speed and direction (**d**).

Table 2. Pearson's correlation between meteorological parameters and pollen disruption in the years 2017 and 2018.

	T_{max} (°C)	T_{min} (°C)	T_{mean} (°C)	Precipt. (mm)	RH (%)	Global Srad (W/m^2)	AtP (hPa)	WS (m/s)	WD (°)	Pollen disr. (%)
T_{max} (°C)	1.000	0.371 *	0.768 *	−0.355 *	−0.573 *	0.672 *	0.549 *	−0.089	−0.360 *	−0.565 *
T_{min} (°C)		1.000	0.188	−0.047	0.010	−0.014	−0.212	−0.105	−0.25	−0.342 *
T_{mean} (°C)			1.000	−0.171	−0.282 *	0.338 *	0.639 *	0.131	−0.350 *	−0.484 *
Precipt.(mm)				1.000	0.535 *	−0.518 *	−0.634 *	−0.083	0.018	0.371 *
RH (%)					1.000	−0.800 *	−0.383	−0.114	0.426 *	0.448 *
Global Srad (W/m^2)						1.000	0.479 *	0.120	−0.214	−0.501 *
AtP (hPa)							1.000	0.048	0.008	−0.519 *
WS (m/s)								1.000	0.024	−0.077
WD (°)									1.000	0.136
Pollen disr. (%)										1.000

* Correlation is significant at 5% ($p < 0.05$); Pollen disr., Pollen disruption; Precipt., Precipitation.

Principal component analysis (PCA) showed that PC1 and PC2 explained approximately 42% and 17% of the total variability of the data, respectively. These two main components explain almost 60% of the variance. PC3 and PC4 allow the explanation of 22% of the total variance (Tables 3 and 4), thus with 4 components, approximately 81% of the total variability of the original data is explained (Table 3). To decide on the number of components to retain, the proportion of variance explained by the components and the eigenvalues of the sample correlation matrix were considered (Table 4).

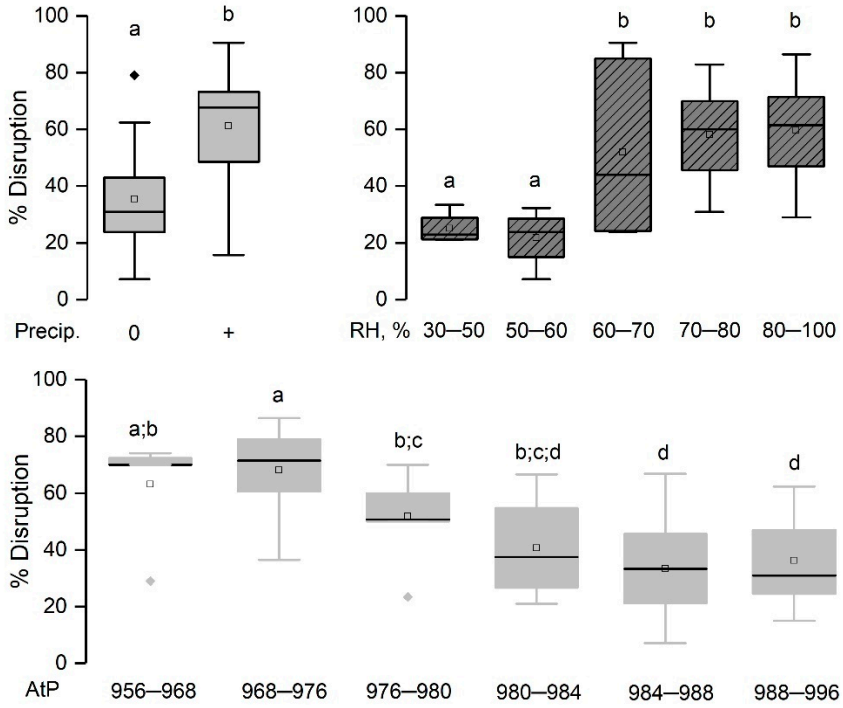

Figure 4. Influence of precipitation, RH and atmospheric pressure (AtP) on pollen disruption. The data was sectioned by the presence or absence of rainfall and by RH and AtP as mentioned. The different letters within the graphs indicate the statistical significance at 5% ($p < 0.05$) among homogeneous subsets.

Table 3. Own values and proportion of variance explained by components.

	Components Variances	Proportion of Variance	Cumulative Proportion
1	4.178	41.78	41.78
2	1.719	17.19	58.97
3	1.165	11.65	70.63
4	1.081	10.81	81.44
5	0.611	6.11	87.55
6	0.539	5.39	92.95
7	0.323	3.23	96.18
8	0.177	1.77	97.96
9	0.144	1.44	99.40
10	0.059	0.59	100

The first main component, PC1, is responsible for the greatest variability in the data. The variables that contributed most to the first component were T_{max}, T_{mean}, precipitation, RH, Global Srad and AtP. For the second component, PC2, the main meteorological parameters were T_{min}, precipitation and WD (Table 4 and Figure 5). All variables, except for WS,

are determinant in the formation of the first two components. WS is the variable with the highest weight in PC4, thus it is the meteorological variable that least contributes to explain the pollen burst (component 4 only explains 11% of the data variability, respectively) (Table 3 and Figure 5). T_{mean}, RH, Global Srad and WD are the main contributors to PC3, however this component contributes to explain only 12% of the data variability. Pollen disruption (%) is associated mainly with PC1.

Table 4. Loadings of principal components.

	PC1	PC2	PC3	PC4
% Pollen disruption	**−0.362**	−0.106	−0.209	0.084
T_{max} (°C)	**0.421**	−0.271	0.170	0.111
T_{mean} (°C)	**0.353**	−0.128	**0.556**	−0.105
T_{min} (°C)	0.019	**−0.665**	0.119	0.070
Precipitation(mm)	**−0.315**	**−0.336**	0.236	−0.290
RH (%)	**−0.379**	0.0315	**0.494**	0.090
GlobalSrad (W/m^2)	**0.398**	0.035	**−0.326**	−0.070
AtP (hPa)	**0.369**	0.279	0.274	0.103
WS (m/s)	0.036	0.106	0.009	**−0.921**
WD (°)	−0.162	**0.499**	**0.346**	0.087

In bold: values are significant (>0.300).

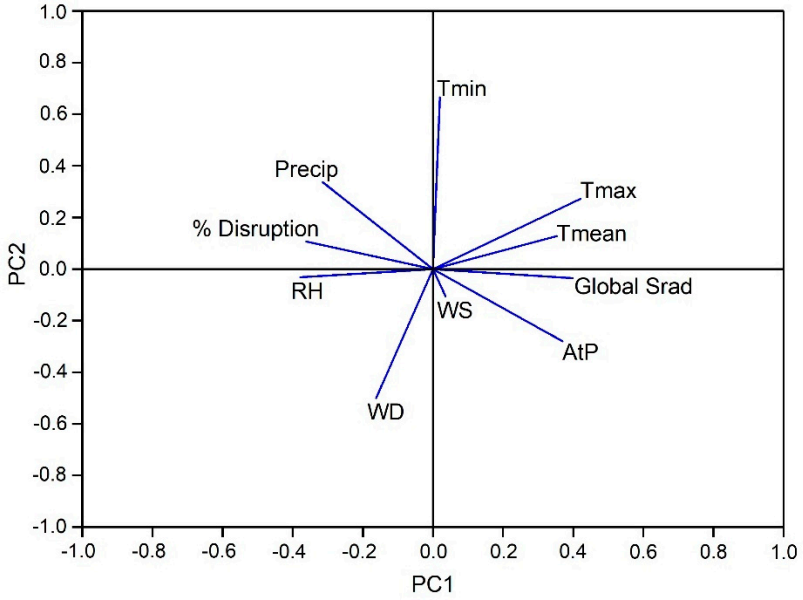

Figure 5. Diagram of the contribution of each variable for PC1 and PC2.

Figure 5 shows that precipitation and RH is positively associated with pollen disruption while AtP, Global Srad and T_{mean} are negatively associated with pollen disruption, according to the correlation analysis.

3.3. Intra-Diurnal Variations of Pollen Concentration and Meteorological Parameters

The diurnal variability of the hourly distribution patterns of Cupressaceae pollen and meteorological parameters were analysed on four days with high and low pollen disruption, within the period studied.

Table 5 depicts the detailed characteristics of the selected days in terms of DPI, pollen disruption, daily averaged temperatures, rainfall, Global Srad, AtP, WS and WD. All days selected have significant DPI and pollen disruption, verifying from 23% to 75%. T_{mean} and

T_{max} were not significantly different. T_{min} was also similar between days except for 27 February 2017; this day presented the lowest T_{max} and the highest T_{min}.

Table 5. Characterization of two days of high and low pollen disruption in the years 2017 and 2018 in Évora.

	25 February 2017	27 February 2017	25 February 2018	26 February 2018
DPC (pollen/m^3)	1635.0	938.0	185.0	644.0
Ruptured pollen (%)	42.5	34.3	23.2	75.3
T_{max} (°C)	18.9	16.9	19.0	18.2
T_{min} (°C)	7.5	10.1	6.7	7.3
T_{mean} (°C)	12.9	12.5	12.3	11.1
Rainfall (mm)	0.0	1.0	0.0	5.4
RH (%)	76.3	75.5	54.1	76.5
Global Srad(W/m^2)	145.1	99.7	209.4	96.0
AtP (hPa)	987.4	987.2	977.4	972.4
WS (m/s)	1.2	1.3	1.9	1.3
WD (°)	W-SW	W-SW	E	NE

RH was similar for three of the days (75.5–76.5%) but was lower on 25 February 2018. Global Srad was approximately twofold higher on dry days (25 February 2017 and 2018) compared to days with rainfall (27 February 2017 and 26 February 2018). In 2017 the AtP was slightly higher compared to 2018. The predominant wind direction was W-SW in 2017 and E and NE in 2018 and WS was mild for all the days, being more intense on 26 February 2018.

The diurnal pollen and meteorological profiles are depicted in Figure 6. The hourly pollen concentration presented in Figure 6 shows a diurnal cycle, starting to increase at about 07h00 UTC, with a peak between 10h00 14h00 UTC, followed by a diminution during the afternoon. The lowest pollen concentrations were detected during nighttime for all days and higher concentrations detected, predominantly, coincident with a diminution of solar radiation, thus decreasing atmospheric mixing and increasing particle concentrations near the surface.

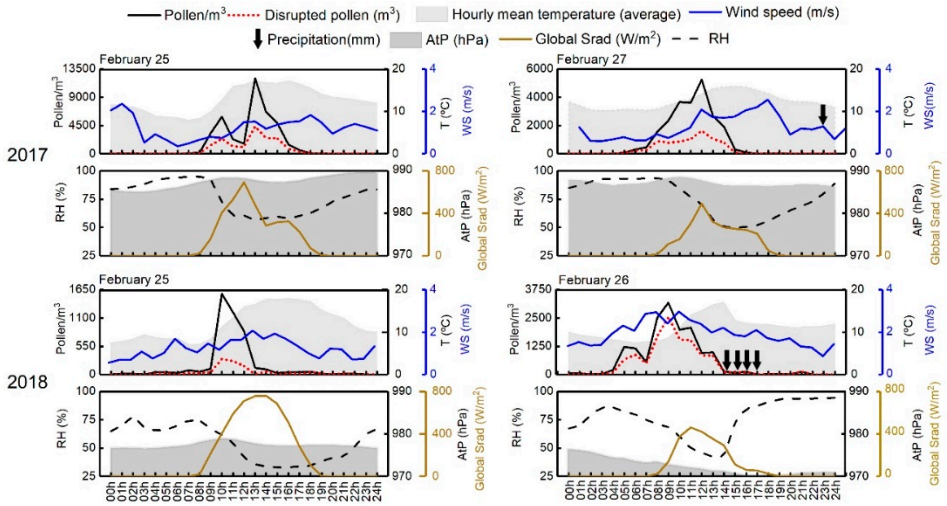

Figure 6. Hourly pollen concentration and meteorological parameters on 4 episodes of high pollen, 2 per year, with high and low pollen disruption indexes.

The maximum pollen peak on the 25 and 27 February 2017, was registered at 13h00 and 12h00, respectively, reaching 11,978 and 5247 pollen/m^3. The pollen concentration began to rise between 07h00 and 08h00 for both days. On 25 and 26 February 2018, the maximum pollen concentration (1568 and 3179 pollen/m^3, respectively) was detected at 10h00 and 09h00, respectively. On 26 February 2018, an additional peak was detected in the period from 04h00 to 07h00, suggesting a long-distance origin (Figure 6).

The variation of mean temperature was similar in the days of analysis, increasing from 9h00 until the middle of the day and then, decreasing again at approximately 19h00. RH was reversed with respect to the mean temperature. Precipitation occurred on 26 February 2018 from 14h00–17h00, coinciding with the decrease in the concentration of pollen in the air, and on 27 February 2017 at 23h00 (Figure 6, 1st and 3rd panels in the right). The atmospheric pressure was higher in 2017 compared to 2018. WS tended to be higher between 10h00 to 19h00, decreasing afterwards in all cases (Figure 6).

The hourly pollen concentration (HPC) was positively and significantly correlated with T and AtP while pollen disruption positively correlated with WS and negatively correlated with AtP (Table 6), suggesting that T and AtP contribute to pollen release and higher WS and lower AtP are factors contributing to pollen integrity loss. It is noteworthy, that the day with the lowest AtP (972.4 hPa) presented the highest disruption ratio (RH = 76.5%); on the contrary, for the day with the lowest disruption ratio the RH was 54.1%, although the AtP was 977.4 hPa (Table 5 and Figure 6).

Table 6. Pearson's correlation between hourly meteorological parameters and hourly disrupted pollen (%) hourly total pollen (m^3).

	T (°C)	RH (%)	Global Srad (W/m^2)	AtP (hPa)	WS (m/s)	Pollen Disruption (%)	HPI (Pollen/m^3)
T (°C)	1.000	−0.701 *	0.848 *	0.395 *	−0.218	−0.225	0.409 *
RH (%)		1.000	−0.785 *	0.262	−0.323	−0.007	−0.109
Global Srad (W/m^2)			1.000	0.147	−0.064	−0.222	0.286
AtP (hPa)				1.000	−0.714 *	−0.587 *	0.407 *
WS (m/s)					1.000	0.451 *	−0.227

* Correlation is significant at the 95% range ($p < 0.05$).

3.4. Remote Sensing and Transport Modelling of Cupressaceae Airborne Pollen: Contribution for Pollen Concentration

The HYSPLIT model was used to estimate the contribution of medium-long range transport of pollen for the DPI in the South of Portugal on the four days selected, at different altitudes (100, 500 and 1000 m). The back trajectories were calculated for every hour of the days analysed. The comparisons showed that for each day there were no significant differences between the results at different times. On the other hand, in most of the cases a pollen peak was observed around 10:00 UTC, therefore these back trajectories were deemed representative of the situation during the rest of the day and are presented in Figure 7. Nevertheless, the hourly trajectories are presented in the Supplementary Materials Figures S2–S5.

Remote sensing data presented aims at supporting the study through the analysis of ceilometer backscatter measurements presented in Figure 8 that are related with the vertical and temporal distribution of aerosols in the lower layers of the atmosphere, since, in the absence of clouds, these particles cause the backscatter sensed by the instrument. These measurements can be used to detect the presence of pollen particles in the atmospheric boundary layer, if there are no other concurrent aerosol events at the same atmospheric levels, such as for example desert dust transports that often occur in the area, which were not detected during the days considered here.

On 25 and 27 February 2017, it was observed from the back trajectory that the air mass came from northwest and west, respectively, passing through continental areas of

central-south Portugal where these species are abundant, as the Sintra mountain and other mountain ranges slightly to the north (Figure 7).

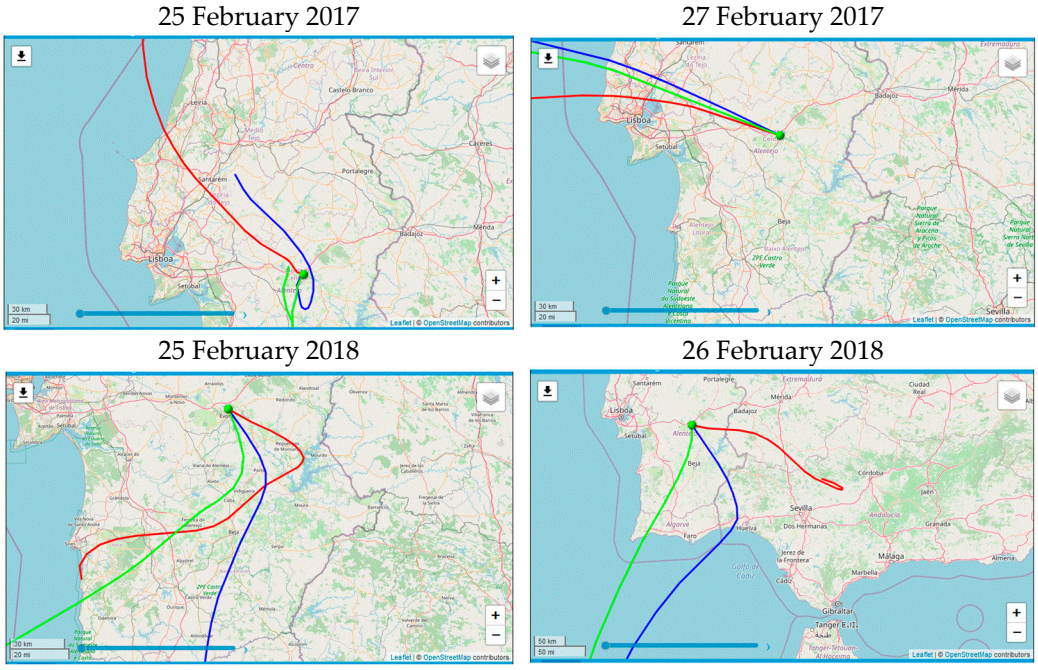

Figure 7. Air mass back trajectory for 2017 and 2018 at 10:00 UTC; height 100 m—red line, height 500 m—blue line and height 1000 m—green line.

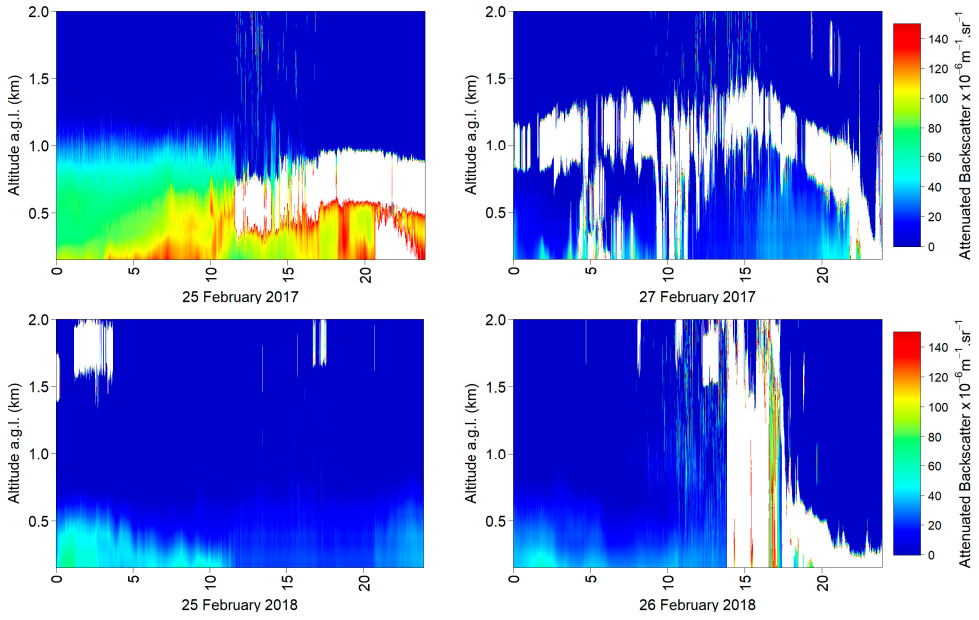

Figure 8. Ceilometer attenuated backscatter on 25 and 27 February 2017 and 25 and 26 February 2018. Clouds are represented in white and are observed over the observatory in the four days.

For the year 2018, on 25 February the back trajectory indicates that the air mass came from the south of Portugal while on 26 February the air mass originated in the southwest coming from south of Spain (Figure 7), where the Cupressaceae family is abundant. On 26 February 2018, a peak was detected between 04h00–06h00 coinciding with air masses originating from southwestern Spain (back trajectory not shown here). The nocturnal period of detection associated with the air mass origin, suggests that these pollens are not

locally originated but regionally transported from Spain. Precipitation occurred in Évora starting at 14h00, coinciding with a decrease of concentration of pollen, due to wash-out and wet deposition.

During the morning (clear sky conditions) of 25 February 2017, only a low layer of particles is distinguished with a moderately high signal. AERONET observations at the same site (not shown here) present a mean aerosol optical depth at 500 nm of 0.31 and mean Ångström exponent of 0.83, typical of relatively large particles. This analysis indicates that the Cupressaceae pollen were probably transported at low levels, below about 1 km, and that their origin matches the regions where these species are mostly concentrated (Figure 8). After 12h00 on 25 February 2017 there were clouds present over the area (white color in the image), which attenuated the signal, hindering the analysis of the vertical distribution of particles in the atmosphere. On 27 February 2017, clouds were present, and the same problems occurred, thus not allowing obtaining a reliable signal of the distribution and intensity of the aerosols, as represented in Figure 8. On 25 and 26 February 2018, the increased backscattered signal at different times indicated the presence of particles at low levels, below about 1 km.

4. Discussion

Cupressaceae pollen, produced in large quantities (523 billion per plant) [38], are considered moderately allergenic [13] and because *Cupressus* species are widely used as ornamental plants, they are widely distributed in urban environments [15], thus being a common cause of winter allergy in urban environments [39], such as Évora, a middle-sized town situated in the South of Portugal. Cupressaceae pollen are present in the atmosphere of Évora during winter–spring, particularly, in the months of February and March (this paper and [11]). In the year 2017, higher concentrations were detected coinciding with higher air temperatures, solar radiation and atmospheric pressure and lower values of relative humidity with respect to 2018. These meteorological conditions can affect the density and viscosity of air [40,41] thus potentially affecting pollen dispersion, resuspension and transport in the atmosphere and, as a consequence the impact on respiratory health of the allergic population.

In this paper we describe a feature of the aerobiology of Cupressaceae pollen characterized by the exine rupture, dilation of intine and sometimes release of the protoplast, as observed in Figure 2a, thus causing the release of pollen allergens and possibly enhancing its allergenic activity. This feature is related to the Cupressaceae pollen morphology characterized for one pore with convex annulus, that has an important role on hydration and exine disruption [42,43]. This event is affected by physical factors during the dispersion process [44] and we have investigated the effect of meteorology factors on this phenomenon on a daily manner and on an intra-diurnal manner.

Concerning the daily observations, the rainfall and relative humidity, particularly above 60%, positively influenced the disruption of the pollen as shown in this paper (Figure 4 and Table 2) and by others. For instance, pollen rupture was reported for *Cupressus arizonica* pollen exposed to water [45], birch pollen exposed to high relative humidity or water [25], and grass pollen subjected to osmotic shock due to high relative humidity or rainwater [26,46] thus releasing the allergen content [47,48]. On the other hand, temperature, global solar radiation and atmospheric pressure are associated with the maintenance of pollen integrity. In fact, PCA analyses show that pollen disruption, rainfall and relative humidity vary in the same manner while atmospheric pressure, temperature and global solar radiation vary together opposing pollen disruption (Figure 5 and Tables 3 and 4). These parameters are all part of the first component that explains most of the variability of the data, in agreement with the correlation analyses. Temperature and global solar radiation relate to relative humidity inversely, indirectly contributing to reduce pollen hydration thus diminishing the probability of pollen disruption. The atmospheric pressure may contribute to counterbalance osmotic pressure, thus opposing the effect of relative humidity and maintaining the pollen integrity while in air suspension. In this paper, the

diurnal pattern of the pollen concentration was evaluated for four selected days. The diurnal pollen profile showed a rise in the morning and a peak at the middle of the day (mostly at 10–12 am) following a pattern described by others [10,20], except for one case on 26 February 2018 where a peak during the night (4–7 am) was observed (Figure 6), coinciding with the thermal inversion period, increased wind speed and decreased relative humidity (Figure 4). These conditions allow anthers dehiscence, pollen emission and dispersion [49]. The increase of relative humidity and the decrease of temperature and wind speed reduce the atmospheric turbulence and enhance pollen deposition [50,51], coinciding with low concentrations of airborne pollen during the afternoon and night. Compared to the daily pollen concentration, the peaks of hourly pollen concentration are 5 to 8 times higher meaning. Hourly pollen concentration reveals that the threshold for allergy reaction might be reached during the day, despite the low daily pollen concentration, thus constituting a more representative human exposure and a better predictor of the risk for allergy outbreaks.

Analysing the effect of meteorological factors on intra-diurnal pollen disruption, while atmospheric pressure is linked to a lower disruption ratio, wind speed correlates with a higher disruption ratio, thus higher release of pollen allergens. Interestingly, hourly relative humidity did not correlate with pollen disruption, opposite of the observations on the daily parameters, nor with hourly pollen concentration. As expected, atmospheric pressure and temperature positively correlate with the hourly pollen concentration (Table 5). Wind speed and atmospheric pressure are correlated and vary inversely as lower surface pressure are frequently associated to low pressure systems where pressure gradients are typically more intense. Hence, the correlation of wind speed with disrupted pollen might be a coincidence following the atmospheric pressure changes. The disruption is a momentary event driven by a disequilibrium between osmotic pressure, generated by relative humidity upon hydration, and atmospheric pressure, pollen bursting occurring when the osmotic pressure overcomes the atmospheric pressure. In this sense, the pollen disruption is a function of the opposing effects of relative humidity and atmospheric pressure. During the four days analysed, the relative humidity was either mainly above or below 60% and atmospheric pressure varied between 972 and 988 hPa. Taking into consideration that 60% relative humidity and 980 hPa are critical values for pollen disruption (Figure 4), then the intra-diurnal variation of atmospheric pressure was the determinant factor for pollen burst, hence the lack of correlation with relative humidity. In fact, the day with the lowest atmospheric pressure associated with a high relative humidity presented the highest disruption ratio. On the contrary, on the day with the lowest disruption ratio the relative humidity was below 60%, despite a low atmospheric pressure (below 980 hPa). For the other days atmospheric pressure above threshold level seems to counterbalance the high relative humidity (Table 5 and Figure 6), supporting the findings on daily observations. Despite the low number of events analysed (4 days), hourly observations revealed a relevant interplay between the key weather factors on airborne pollen integrity loss and a wider research should be carried out in the future to further analyse this phenomenon. Furthermore, it suggests that the period of the day between 10 and 16h is commonly the one with higher risk for exposure to Cupressaceae allergens, as observed for other pollen types [10,20,52,53]. To our knowledge this is the first time that this analysis was performed, unravelling new features of the action of the meteorological factors on pollen behaviour in the atmosphere that might be taken into account for the interpretation of its allergenic potency.

Pollen grains can be deposited elsewhere away from the site that gave rise to it. The pollen grains are small in size and are lightweight and its transport in air masses from long distances was demonstrated for several pollen types [25,54–56] and the intra-diurnal pattern of pollen concentration is an indicator of the contribution of local emission and long range transport to the daily pollen concentration [19,20,53]. Although our results suggest that, for the days analysed, the pollen were mostly from local origin, it was shown that Cupressaceae pollen can be transported long distances in air masses, evidenced by the peak detected at night on 26 February 2018 (Figure 6), that was transported by air masses

passing by the south of Spain, the Andalucia region where Cupressaceae is abundant [57], as suggested by the back trajectory analysis (not shown here). Hence the contribution of medium and long-range transport of Cupressaceae pollen for daily and hourly pollen concentrations cannot be excluded. Based on our results, pollen disruption associated with this transport was not different from the local pollen, but more data will be needed to confirm this observation.

Although clouds were present in all four days considered, in general it can be seen that the remote sensing observations agree with the pollen concentration intra-diurnal behavior, showing concordant daily patterns and backscatter values proportional to the pollen concentrations, which hints that ceilometer measurements may constitute a real-time proxy of the pollen concentration. Note that the remote sensing measurements are instantaneous, with a time resolution of 10 s, whereas the hourly pollen concentration corresponds to a period of one hour (previous 60 min). The case of 25 February 2017 when very high pollen concentrations were detected, with the hourly pollen concentration presenting a secondary peak at around 10:00 UTC and a primary peak at 13:00 UTC, is a good example. The corresponding ceilometer image shows the highest attenuated backscatter values in comparison to the other three days and although clouds are present from 12:00 UTC on (white color in the image), high backscatter values are detected in the lower layers of the atmosphere shortly after 05:00 until about 12:00, when clouds obstruct the particle backscatter detection. It is noteworthy, that on 25 February 2017, the pollen peak at 13h (Figure 6, upper panel) is consistent with a sudden diminution of solar radiation caused by clouds over the area (Figure 8), which induced changes in atmospheric turbulence and mixing, and a probable decrease of the atmospheric boundary layer height and increase of particles near the collector. In this period of analysis, no precipitation occurred. The temperature increased and the relative humidity was approximately 80% (Table 4). On 27 February 2017 the presence of clouds during the whole day does not allow for the analysis. On 25 (26) February 2018, the increased backscatter between 08:00 and 12:00 UTC (03:00 and 14:00 UTC) agrees well with the corresponding hourly pollen concentration shown in Figure 6. On 25 February 2018, the atmospheric boundary layer shows increased backscatter values shortly after midnight, which may be due to the lower thickness of this layer during nighttime with respect to daytime and the existence of non- biological particles [51].

This analysis agrees with findings of several authors in studies related to the detection of particles from remote sensing instruments, demonstrating that this technique can be used to detect the presence of aerosols, more specifically pollen in the atmospheric boundary layer [50,58,59]. As demonstrated by hourly pollen concentrations (this work and [60,61], the real-time pollen concentration to which the population is exposed during the day, is significantly higher than the daily estimates. Remote sensing combined with back trajectories and the other relevant meteorological parameters may in the future contribute to develop real-time methodologies for the detection of pollen in the atmosphere as well as allergy risk warning systems contributing to improve allergy management strategies.

In summary, the results shown in this paper suggest that relative humidity, rainfall and atmospheric pressure are the main factors affecting airborne Cupressaceae pollen integrity and in conjunction with the pollen concentration may be used to predict the risk of allergy outbreaks to this pollen type.

5. Conclusions

To our knowledge, this is the first report characterizing the considerable fraction of disrupted Cupressaceae pollen grains reaching the sampler, releasing pollen contents. It is expected that this disruption might significantly increase ambient free allergen, contributing to enhance ambient allergenic activity of this pollen type because of higher allergen availability. Moreover, this free allergen, contained most probably in small particles, readily inhaled, and might penetrate in the lower respiratory system thus evoking aggravated symptoms in sensitized individuals.

A better knowledge of the factors affecting pollen disruption of allergenic species will greatly contribute to improve allergy risk management. This work significantly contributes to a better understanding of this phenomenon, where relative humidity, atmospheric pressure and rainfall are key players. Being widely used as ornamental plants, *Cupressus* genera are widely distributed in urban environments or its surroundings, and this work also shows that Cupressaceae pollen was mainly from local origin, thus suggesting for a wise planning of urban gardens and green zones, contributing to diminish the loads of allergenic pollen.

Finally, the real-time pollen monitoring, namely by remote sensing, and the relevant meteorological parameters, may contribute to the development of pollen allergy forecasts and thus to a better management of allergy and asthma outbreaks.

Supplementary Materials: The following are available online at https://www.mdpi.com/1999-4907/12/1/64/s1, Figure S1: Regression analysis of the daily disrupted pollen in relation to the daily pollen in 2017 and 2018 together (**a**) and separately (**b**). The data corresponds to the number of pollen grains counted per day (N), Figure S2: Hourly air mass back trajectories for 25 February 2017; height 100 m–red line, height 500 m–blue line and height 1000 m–green line, Figure S3: Hourly air mass back trajectories for 27 February 2017; height 100 m–red line, height 500 m–blue line and height 1000 m–green line, Figure S4: Hourly air mass back trajectories for 25 February 2018; height 100 m–red line, height 500 m–blue line and height 1000 m–green line, Figure S5: Hourly air mass back trajectories for 26 February 2018; height 100 m–red line, height 500 m–blue line and height 1000 m–green line.

Author Contributions: All the authors actively and significantly contributed to this manuscript, as follows: Conceptualization, A.G. and C.M.A.; methodology, A.G., M.J.C. and D.B.; validation, A.G., A.R.C., C.M.A., M.J.C. and R.A.-J.; formal analysis, A.G., A.R.C., C.M.A., M.J.C. and R.A.-J.; investigation, A.G.; resources, C.M.A., A.R.C. and M.J.C.; data curation, A.G., C.M.A. and M.J.C.; writing—original draft preparation, A.G., A.R.C. and M.J.C.; writing—review and editing, C.M.A., D.B., M.J.C., R.S., R.A.-J.; visualization, A.G., A.R.C.; C.M.A., D.B., M.J.C.; supervision, C.M.A.; project administration, C.M.A., A.R.C. and M.J.C.; funding acquisition, A.R.C., C.M.A., D.B., M.J.C. and R.S. All authors have read and agreed to the published version of the manuscript.

Funding: The work is financed by national funds through FCT—Foundation for Science and Technology, I.P., within the scope of the projects UIDB/04683/2020 e UIDP/04683/2020 and also through projects TOMAQAPA (PTDC/CTAMET/ 29678/2017) and NanoSen-AQM (SOE2/P1/E0569)—EU-INTERREG-SUDOE; COST CA18226 "ADOPT- New approaches in detection of pathogens and aeroallergens" and COST CA18235—"PROBE-PROfiling the atmospheric Boundary layer at European scale". Supported by the European Commission, COST Office AUTOPOLLEN—EIG EUMETNET "Proof-of-Concept for a European automatic pollen monitoring network using high temporal-resolution real-time measurements".

Institutional Review Board Statement: Not applicable.

Informed Consent Statement: Not applicable.

Data Availability Statement: Publicly available datasets of meteorological data were analyzed in this study. These data can be found here: [https://www.icterra.pt/g1/index.php/meteo-data/]; Pollen datasets are accessible either in [https://lince.di.uevora.pt/polen/index.jsp] upon request and within this article.

Acknowledgments: The authors gratefully acknowledge the NOAA Air Resources Laboratory (ARL) for the provision of the HYSPLIT transport and dispersion model and/or READY website (https://www.ready.noaa.gov) used in this publication.

Conflicts of Interest: The authors declare no conflict of interest.

References

1. Schulz, C.; Knopf, P.; Stützel, T. Identification key to the Cypress family (Cupressaceae). *Feddes Repert.* **2005**, *116*, 96–146. [CrossRef]
2. Christenhusz, M.J.M.; Reveal, J.L.; Farjon, A.; Gardner, M.F.; Mill, R.R.; Chase, M.W. A new classification and linear sequence of extant gymnosperms. *Phytotaxa* **2011**, *19*, 55–70. [CrossRef]
3. Farjon, A. The Kew Review: Conifers of the World. *Kew Bull.* **2018**, *73*, 8. [CrossRef]

4. San-Miguel-Ayanz, J.; de Rigo, D.; Caudullo, G.; Houston Durrant, T.; Mauri, A.; Tinner, W.; Ballian, D.; Beck, P.; Birks, H.J.B.; Eaton, E.; et al. *European Atlas of Forest Tree Species*; San-Miguel-Ayanz, J., de Rigo, D., Caudullo, G., Houston Durrant, T., Mauri, A., Eds.; Publication Office of the European Union: Luxembourg, 2016; ISBN 978-92-79-36740-3.
5. Instituto da Conservação da Natureza e das Florestas. I.P. Instituto de Conservação da Natureza e das Florestas. Available online: https://www.icnf.pt/ (accessed on 1 September 2020).
6. Sociedade Portuguesa de Botânica Flora-On: Flora de Portugal Interactiva. Available online: https://flora-on.pt/ (accessed on 21 December 2020).
7. Universidade de Trás-os-Montes e Alto Douro Jardim Botânico UTAD. Available online: https://jb.utad.pt/ (accessed on 21 December 2020).
8. Hidalgo, P.J.; Galán, C.; Domínguez, E. Male phenology of three species of Cupressus: Correlation with airborne pollen. *Trees Struct. Funct.* **2003**, *17*, 336–344. [CrossRef]
9. Khanduri, V.P.; Sharma, C.M. Development of groups of male strobili, anthesis and microsporangium dehiscence in Pinus roxburghii. *Grana* **2000**, *39*, 169–174. [CrossRef]
10. Guardia, C.; Alba-Sánchez, F.; De Linares, C.; Nieto-Lugilde, D.; Caballero, J. Aerobiological and allergenic analysis of Cupressaceae pollen in Granada (Southern Spain). *JIACI J. Investig. Allergol. Clin. Immunol.* **2006**, *16*, 24–33.
11. Caeiro, E.; Penedos, C.; Carreiro-Martins, P.; Nunes, C.; Almeida, M.M.; Pedro, E.; Rodrigues-Alves, R.; Ferreira, M.B. Aerobiologia do pólen de Cupressáceas em Portugal. *Rev. Port. Imunoalergologia* **2020**, *28*, 19–30. [CrossRef]
12. Antunes, C.M.; Costa, A.R.; Galveias, A.; Ribeiro, H.; Abreu, I.; Rodrigues, P.; Deus, R.; Saias, J. Pólen Alert. Available online: https://lince.di.uevora.pt/polen/index.jsp (accessed on 1 September 2020).
13. Boutin-Forzano, S.; Gouitaa, M.; Hammou, Y.; Ramadour, M.; Charpin, D. Personal risk factors for cypress pollen allergy. *Allergy Eur. J. Allergy Clin. Immunol.* **2005**, *60*, 533–535. [CrossRef]
14. D'Amato, G.; Cecchi, L.; Bonini, S.; Nunes, C.; Annesi-Maesano, I.; Behrendt, H.; Liccardi, G.; Popov, T.; Van Cauwenberge, P. Allergenic pollen and pollen allergy in Europe. *Allergy Eur. J. Allergy Clin. Immunol.* **2007**, *62*, 976–990. [CrossRef]
15. Perez-Badia, R.; Rapp, A.; Morales, C.; Sardinero, S.; Galan, C.; Garcia-Mozo, H. Pollen Spectrum and Risk of pollen allergy in central spain. *Ann. Agric. Environ. Med.* **2010**, *17*, 139–151.
16. Rodriguez, O.; Célio, R.; Aboukhair, F.; Laurrabaquio, A.M.; Tinoca, I.T.; Cuevas, H.U.; Cruz Suaréz, M.A.; Cruz Marmolejo, M.A.; Reyes, M.C. Prueba cutánea con extractos alergénicos de pólenes y relación con signos clínicos de rinitis alérgica y asma bronquial en Camagüey, Cuba. *Vaccimonitor* **2013**, *22*, 9–13.
17. Guerra, F.; Daza, J.C.; Miguel, R.; Moreno, C.; Galán, C.; Domínguez, E.; Sánchez Guijo, P. Sensitivity to Cupressus: Allergenic significance in Córdoba (Spain). *J. Investig. Allergol. Clin. Immunol.* **1996**, *6*, 117–120.
18. Laaidi, M. Forecasting the start of the pollen season of Poaceæ: Evaluation of some methods based on meteorological factors. *Int. J. Biometeorol.* **2001**, *45*, 1–7. [CrossRef] [PubMed]
19. Galán, C.; Tormo, R.; Cuevas, J.; Infante, F.; Domínguez, E. Theoretical daily variation patterns of airborne pollen in the south-west of Spain. *Grana* **1991**, *30*, 201–209. [CrossRef]
20. Ribeiro, H.; Oliveira, M.; Abreu, I. Intradiurnal variation of allergenic pollen in the city of Porto (Portugal). *Aerobiologia* **2008**, *24*, 173–177. [CrossRef]
21. Tortajada, B.; Mateu, I. Concentraciones de polen de cupresáceas en la atmósfera de Valencia (Este de España) y su relación con los parámetros meteorológicos—Dialnet. *Polen* **2008**, *18*, 51–59.
22. Aira, M.J.; Dopazo, A.; Jato, M.V. Aerobiological monitoring of Cupressaceae pollen in Santiago de Compostela (NW Iberian Peninsula) over six years. *Aerobiologia* **2001**, *17*, 319–325. [CrossRef]
23. Taylor, P.E.; Flagan, R.C.; Valenta, R.; Glovsky, M.M. Release of allergens as respirable aerosols: A link between grass pollen and asthma. *J. Allergy Clin. Immunol.* **2002**, *109*, 51–56. [CrossRef]
24. Taylor, P.E.; Flagan, R.C.; Miguel, A.G.; Valenta, R.; Glovsky, M.M. Birch pollen rupture and the release of aerosols of respirable allergens. *Clin. Exp. Allergy* **2004**, *34*, 1591–1596. [CrossRef]
25. Galán, C.; Antunes, C.; Brandao, R.; Torres, C.; Garcia-Mozo, H.; Caeiro, E.; Ferro, R.; Prank, M.; Sofiev, M.; Albertini, R.; et al. Airborne olive pollen counts are not representative of exposure to the major olive allergen Ole e 1. *Allergy* **2013**, *68*, 809–812. [CrossRef]
26. Thien, F.; Beggs, P.J.; Csutoros, D.; Darvall, J.; Hew, M.; Davies, J.M.; Bardin, P.G.; Bannister, T.; Barnes, S.; Bellomo, R.; et al. The Melbourne epidemic thunderstorm asthma event 2016: An investigation of environmental triggers, effect on health services, and patient risk factors. *Lancet Planet. Health* **2018**, *2*, e255–e263. [CrossRef]
27. Instituto Português do Mar e da Atmosfera. Available online: http://www.ipma.pt/pt/index.html/ (accessed on 30 November 2020).
28. Galán Soldevilla, C. *Spanish Aerobiology Network (REA): Management and Quality Manual*; Servicio de Publicaciones, Universidad de Córdoba: Córdoba, Spain, 2007; ISBN 9788469063538.
29. Galán, C.; Smith, M.; Thibaudon, M.; Frenguelli, G.; Oteros, J.; Gehrig, R.; Berger, U.; Clot, B.; Brandao, R. Pollen monitoring: Minimum requirements and reproducibility of analysis. *Aerobiologia* **2014**, *30*, 385–395. [CrossRef]
30. Nilsson, S.; Persson, S. Tree pollen spectra in the stockholm region (sweden), 1973–1980. *Grana* **1981**, *20*, 179–182. [CrossRef]
31. Andersen, T.B. A model to predict the beginning of the pollen season. *Grana* **1991**, *30*, 269–275. [CrossRef]

32. Scientific Campbell CR1000 Measurement and Control System. Available online: https://s.campbellsci.com/documents/br/manuals/cr1000.pdf (accessed on 21 December 2020).
33. Stein, A.F.; Draxler, R.R.; Rolph, G.D.; Stunder, B.J.B.; Cohen, M.D.; Ngan, F. NOAA's HYSPLIT Atmospheric Transport and Dispersion Modeling System. *Bull. Am. Meteorol. Soc.* **2016**, *96*, 2059–2077. [CrossRef]
34. Rolph, G.; Stein, A.; Stunder, B. Real-time Environmental Applications and Display sYstem: READY. *Environ. Model. Softw.* **2017**, *95*, 210–228. [CrossRef]
35. Zar, J.H. *Biostatistical Analysis*, 5th ed.; Prentice Hall: Upper Saddle River, NJ, USA, 2007.
36. Johnson, R.A.; Wichern, D.W. *Applied Multivariate Statistical Analysis*; Prentice Hall: Upper Saddle River, NJ, USA, 2002; Volume 5.
37. Palma, P.; Fialho, S.; Lima, A.; Novais, M.H.; Costa, M.J.; Montemurro, N.; Pérez, S.; de Alda, M.L. Pharmaceuticals in a Mediterranean Basin: The influence of temporal and hydrological patterns in environmental risk assessment. *Sci. Total Environ.* **2020**, *709*, 136205. [CrossRef]
38. Bunderson, L.D.; de Water, P.; Wells, H.; Levetin, E. Predicting and quantifying pollen production in Juniperus ashei forests. *Phytologia* **2012**, *94*, 417–438.
39. Charpin, D.; Pichot, C.; Belmonte, J.; Sutra, J.P.; Zidkova, J.; Chanez, P.; Shahali, Y.; Sénéchal, H.; Poncet, P. Cypress Pollinosis: From Tree to Clinic. *Clin. Rev. Allergy Immunol.* **2019**, *56*, 174–195. [CrossRef]
40. Tsilingiris, P.T. Thermophysical and transport properties of humid air at temperature range between 0 and 100 °C. *Energy Convers. Manag.* **2008**, *49*, 1098–1110. [CrossRef]
41. Gregory, P.H. Distribution of airborne pollen and spores and their long distance transport. *Pure Appl. Geophys.* **1978**, *116*, 309–315. [CrossRef]
42. Duhoux, E. Mechanism of exine rupture in hydrated taxoid type of pollen. *Grana* **1982**, *21*, 1–7. [CrossRef]
43. Bortenschlager, S. Aspects of pollen morphology in the cupressaceae. *Grana* **1990**, *29*, 129–138. [CrossRef]
44. Sofiev, M.; Belmonte, J.; Gehrig, R.; Izquierdo, R.; Smith, M.; Dahl, A.; Siljamo, P. Airborne pollen transport. In *Allergenic Pollen: A Review of the Production, Release, Distribution and Health Impacts*; Springer: Dordrecht, The Netherlands, 2013; Volume 9789400748811, pp. 127–159. ISBN 9789400748811.
45. Chichiriccò, G.; Pacini, E. *Cupressus arizonica* pollen wall zonation and in vitro hydration. *Plant Syst. Evol.* **2008**, *270*, 231–242. [CrossRef]
46. Knox, R.B. Grass pollen, thunderstorms and asthma. *Clin. Exp. Allergy J. Br. Soc. Allergy Clin. Immunol.* **1993**, *23*, 354–359. [CrossRef] [PubMed]
47. Buters, J.; Prank, M.; Sofiev, M.; Pusch, G.; Albertini, R.; Annesi-Maesano, I.; Antunes, C.; Behrendt, H.; Berger, U.; Brandao, R.; et al. Variation of the group 5 grass pollen allergen content of airborne pollen in relation to geographic location and time in season the HIALINE working group. *J. Allergy Clin. Immunol.* **2015**, *136*, 87–95. [CrossRef]
48. Aloisi, I.; Del Duca, S.; De Nuntiis, P.; Vega Maray, A.M.; Mandrioli, P.; Gutiérrez, P.; Fernández-González, D. Behavior of profilins in the atmosphere and in vitro, and their relationship with the performance of airborne pollen. *Atmos. Environ.* **2018**, *178*, 231–241. [CrossRef]
49. Cresti, M.; Linskens, H.F. Pollen-allergy as an ecological phenomenon: A review. *Plant Biosyst.* **2000**, *134*, 341–352. [CrossRef]
50. Sicard, M.; Izquierdo Miguel, R.; Alarcón Jordán, M.; Belmonte Soler, J.; Comerón Tejero, A.; Baldasano Recio, J.M. Near-surface and columnar measurements with a micro pulse lidar of atmospheric pollen in Barcelona, Spain. *Atmos. Chem. Phys.* **2016**, *16*, 6805–6821. [CrossRef]
51. Malico, I.; Pereira, S.N.; Costa, M.J. Black carbon trends in southwestern Iberia in the context of the financial and economic crisis. The role of bioenergy. *Environ. Sci. Pollut. Res.* **2017**, *24*, 476–488. [CrossRef]
52. Fernández-Rodríguez, S.; Maya-Manzano, J.M.; Colín, A.M.; Pecero-Casimiro, R.; Buters, J.; Oteros, J. Understanding hourly patterns of Olea pollen concentrations as tool for the environmental impact assessment. *Sci. Total Environ.* **2020**, *736*, 139363. [CrossRef] [PubMed]
53. Rojo, J.; Rapp, A.; Lara, B.; Fernández-González, F.; Pérez-Badia, R. Effect of land uses and wind direction on the contribution of local sources to airborne pollen. *Sci. Total Environ.* **2015**, *538*, 672–682. [CrossRef] [PubMed]
54. Levetin, E. A long-term study of winter and early spring tree pollen in the Tulsa, Oklahoma atmosphere. *Aerobiologia* **1998**, *14*, 21–28. [CrossRef]
55. Mohanty, R.P.; Buchheim, M.A.; Anderson, J.; Levetin, E. Molecular analysis confirms the long-distance transport of Juniperus ashei pollen. *PLoS ONE* **2017**, *12*, e0173465. [CrossRef]
56. Rogers, C.A.; Levetin, E. Evidence of long-distance transport of mountain cedar pollen into Tulsa, Oklahoma. *Int. J. Biometeorol.* **1998**, *42*, 65–72. [CrossRef]
57. Docampo, S.; Recio, M.; Trigo, M.M.; Melgar, M.; Cabezudo, B. Risk of pollen allergy in Nerja (southern Spain): A pollen calendar. *Aerobiologia* **2007**, *23*, 189. [CrossRef]
58. Sassen, K. Boreal tree pollen sensed by polarization lidar: Depolarizing biogenic chaff. *Geophys. Res. Lett.* **2008**, *35*, L18810. [CrossRef]
59. Bohlmann, S.; Shang, X.; Giannakaki, E.; Filioglou, M.; Saarto, A.; Romakkaniemi, S.; Komppula, M. Detection and characterization of birch pollen in the atmosphere using a multiwavelength Raman polarization lidar and Hirst-type pollen sampler in Finland. *Atmos. Chem. Phys.* **2019**, *19*, 14559–14569. [CrossRef]

60. Shang, X.; Giannakaki, E.; Bohlmann, S.; Filioglou, M.; Saarto, A.; Ruuskanen, A.; Leskinen, A.; Romakkaniemi, S.; Komppula, M. Airborne pollen observations using a multi-wavelength Raman polarization lidar in Finland: Characterization of pure pollen types. *Atmos. Chem. Phys. Discuss.* **2020**. [CrossRef]
61. Richardson, S.C.; Mytilinaios, M.; Foskinis, R.; Kyrou, C.; Papayannis, A.; Pyrri, I.; Giannoutsou, E.; Adamakis, I.D.S. Bioaerosol detection over Athens, Greece using the laser induced fluorescence technique. *Sci. Total Environ.* **2019**, *696*, 133906. [CrossRef]